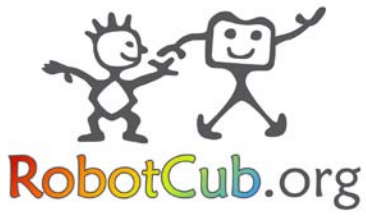

ROBotic Open-architectureTechnology for Cognition, Understanding and Behavior

Project no. 004370

RobotCub: Development of a cognitive humanoid cub

Instrument: Integrated Project
Thematic Priority: IST – Cognitive Systems

D3.7 Human Electrophysiology: Preliminary Data

Due Date: 31/08/2009
Submission date: End of the Project

Start date of project: **01/09/2004** Duration: **60+5 months**

Organisation name of lead contractor for this deliverable: UNIFE

Responsible Person: Prof. Luciano Fadiga

Revision: **1.1**

Project co-funded by the European Commission within the Sixth Framework Programme (2002-2006)		
Dissemination Level		
PU	Public	**PU**
PP	Restricted to other programme participants (including the Commission Service)	
RE	Restricted to a group specified by the consortium (including the Commission Service)	
CO	Confidential, only for members of the consortium (including the Commission Service)	

Table of Contents

1 Introduction

The large majority of empirical evidence about the existence of sensorimotor neurons (Fadiga et al., 2000. See also RobotCub Deliverable 3.1) comes from animal models, more frequently macaque monkeys. It is therefore still correlational the conclusion that similar mechanisms exist and work in the human brain. In fact, the neurophysiology of the human cerebral cortex is mainly based on brain imaging techniques based on the measurement of regional blood flow (Positron Emission Tomography, PET; functional Magnetic Resonance Imaging, fMRI) and on electrophysiological techniques masuring the electrical activity of huge neuronal populations (Electroencephalography, EEG; Elettrocorticography, ECoG; Magnetoencephalography, MEG). Both types of techniques have severe limitation either because of poor temporal or spatial resolution. Although there is large consent about the existence of a correlation between neuronal activity modifications and parallel modifications of regional blood flow (which is the signal at the basis of PET and fMRI), it is not completely clear which neural mechanisms are responsible for such blood flow modulation. Present evidence suggests that the responsibility of blood flow modifications should be attributed not only to neurons' action potentials, but also to presynaptic activation (without the possibility, therefore, to clearly distinguish between excitation- and inhibition-induced effects). The aim of the present project is to address this problem by associating brain imaging techniques (as fMRI) to extracellular recordings of single neuron (a direct measure of the neuron's output).

The recording of single neurons in humans has been rarely performed and almost exclusively in pathological brain parts during the neurosurgical treatment of epilepsy. On the contrary, the present study starts from the unique opportunity that derives from the collaboration existing between the Neurosurgery Division of Udine Hospital, the Ferrara University and the Italian Institute of Technology, to study the border of brain cancers by electrophysiological techniques (i.e., single neurons). The possibility to record single neuron activity in awake humans will give essential elements to reveal the intimate mechanisms of sensorimotor integration in humans: before surgery, patients are investigated by using functional magnetic resonance imaging (fMRI) and high resolution electroencephalography (hr-

EEG), during sensorimotor and cognitive tasks that are specifically selected according to the lesion site (e.g., if the lesion is located close to the hand representation of the primary motor cortex, the task will require hand mobilization, sensory stimulation, hand action observation, etc.). During surgery, similar tasks are performed by patients (during single unit recordings) giving therefore the terms for the comparison between the results arising from the different techniques. Our aim is to provide physiological data about cortical areas that until now have been rarely studied with microelectrode-based electrophysiological techniques. This is because, in our approach, neurophysiology is at the service of the patient: Intracortical recordings of single neuron activity in patients with low-grade gliomas allow to determine the functional border between pathological and normal brain tissue. In the specific case of low-grade lesions it is mandatory to define an acceptable compromise between the extension of the surgical ablation (that determines *quod vitam* prognosis) and the possible consequent functional deficit (that determines *quod functionem* prognosis). For these reasons, the Ethical Committee of Udine Hospital has expressed a positive judgment about this project and its finalities.

The low-grade glioma is a type of brain tumour that does not spread outside the brain, not malignant during early development (Guthrie and Laws 1990). Then, as the tumour mass increases, gliomas degenerate towards malignant forms (Nakamura, Konishi et al. 2000). They slowly infiltrate the brain, often causing epileptic seizures, and their borders with the healthy tissue are poorly defined. Because of that, many low-grade gliomas are surgically removed and the larger extent of resection seems to correlate with an improved outcome (Sanai and Berger, 2008). Since any damage in healthy brain areas may result into postoperative disturbances thus greatly reduce surgery benefits, intraoperative functional brain mapping techniques are used to delineate tumor borders (Berger and Rostomily 1997; Duffau, Capelle et al. 2003; Neuoloh, Pechstein et al. 2004). Although the intraoperative stimulation mapping in an awake patients is considered the gold standard for delineation of functional brain areas (Duffau, Capelle et al. 2003), other intraoperative functional mapping methods such as motor evoked potentials (Neuoloh, Pechstein et al. 2004), EEG and electrocorticograms (Berger, Ghatan et al. 1993) are also used. Recently, we have shown that single unit recordings can aid mapping procedures by identifying brain areas that show normal activity and respond with change in their neuronal

activity when a patient performs some actions such as speech, hand movement or is presented with visual stimuli (Bonfanti et al., 2009).

To record single- and multi-units with microelectrode arrays during tumour resection, we developed a compact 8/16-channel single- and multi-unit recording system suitable for the use in surgery room. The system includes a computer-controlled motor drive with an autoclavable headstage. All control units including the signal digitization board are mounted in a single rack, while the headstage comprises an integrated 8 channel amplifier with two motor drives, one for the microelectrode insertion and the second one to control the pressure exerted by the headstage on the brain. All system components are powered from batteries. The acquired signal quality is comparable to the best commercial multichannel. We successfully tested this system in a human surgery room. Laboratory tests show that such a system is relatively easy to scale to up to 64 channels.

2 Methods

This deliverable describes some technological advancements allowing safe and reliable recordings of single neurons in awake human subjects. This methodological part is subdivided into two sections. The first section describes the general methodology followed before and during the neurosurgery, the second describes the system we set up in collaboration with IIT to perform single neuron recordings in the awake, collaborating patient.

General Methodology.

Subjects. 245 Patients (84% right handed, 104 females, 150 males; mean age, 46.5). About 75% were affected by low-grade and high-grade gliomas. The remaining lesions were vascular (4%), meningiomas (8%), metastasis (10%) and others (3%). Twenty-two patients have been submitted until now to the single neurons recording procedure.

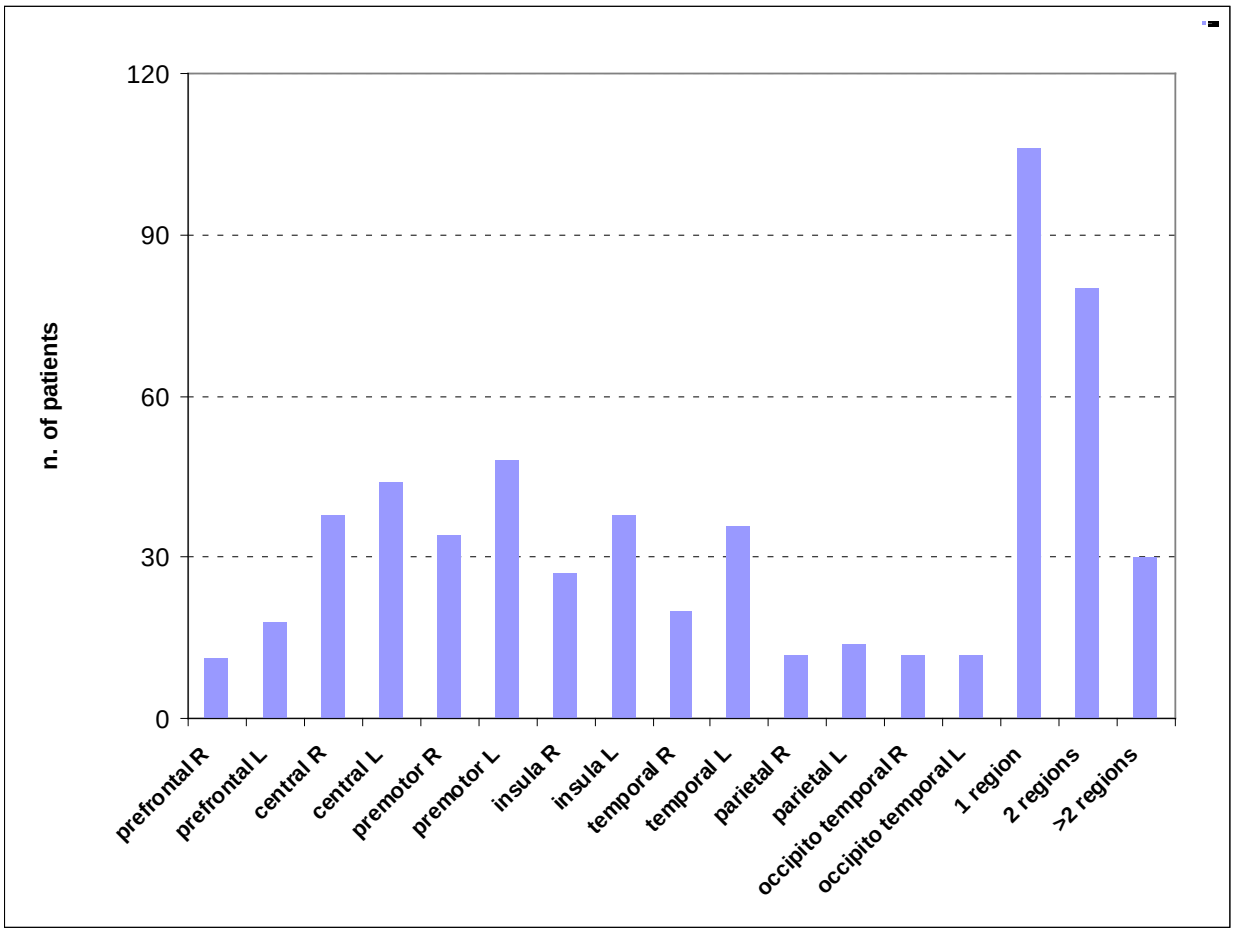

Figure 1. Anatomical localization of patients' lesion. Note the large prevalence of frontal (motor and premotor) sites.

Neuropsychological testing. Patients have been submitted to neuropsychological screening to evaluate their cognitive abilities using a number of tests selected on the basis of lesion localization. Handedness has been measured in all of the patients. In addition to that, the neuropsychological screening for: (1) Left hemisphere patients: Language-related abilities, verbal short- and long- term memory and imitation of symbolic and meaningless upper limb gestures. (2) Right hemisphere patients: visuo-spatial abilities: e.g., neglect, figure copying, measures of spatial short-term memory. (3) Patients with anterior lesions were additionally tested for their verbal fluency e trial making tests. (4) Patients with posterior lesions were additionally tested for the presence of visual agnosia and, in some cases, were submitted to the *Visual Object and Space Perception Battery* (i.e., VOSP, see Warrington and James, 1991).

fMRI acquisition and analysis. Acquisition. Functional axial images (Siemens Avanto 1.5 T, 16 channels coil), T2*-weighted gradient-echo echo planar imaging (EPI) sequence (echo time TE = 60 ms, repetition time TR = 3000 ms, flip-angle 90°, in-plane resolution 3.28 mm x 3.28 mm), covering the whole brain (30 contiguous 5 mm slices per volume). 45 volumes per run (the first 3 volumes discarded to reach the steady state magnetic saturation). T1*-weighted structural images also acquired (MP-RAGE sequence, TE = 2.86 ms, TI = 1100 ms, repetition time TR = 2300 ms, flip-angle 20°, isotropic voxel with 1 x 1 x 1 mm). Analysis: fMRI data were analyzed using FSL software (Analysis Group, FMRIB, Oxford, UK -http://www.fmrib.ox.ac.uk/fsl) after correction for differences in acquisition timing, spatial realignment, smoothing (Gaussian kernel, 3 mm FWHM), high-pass filtering (30 s), corrected for temporal autocorrelation. Functional data were analyzed using a general linear model approach. Regressors of Block-related BOLD responses were modeled in each patient from each trial type using a standard hemodynamic response function. To obtain statistical maps overlaid on the T1 with contrast high resolution anatomical images the mean EPI image was co-registered with the anatomical one.

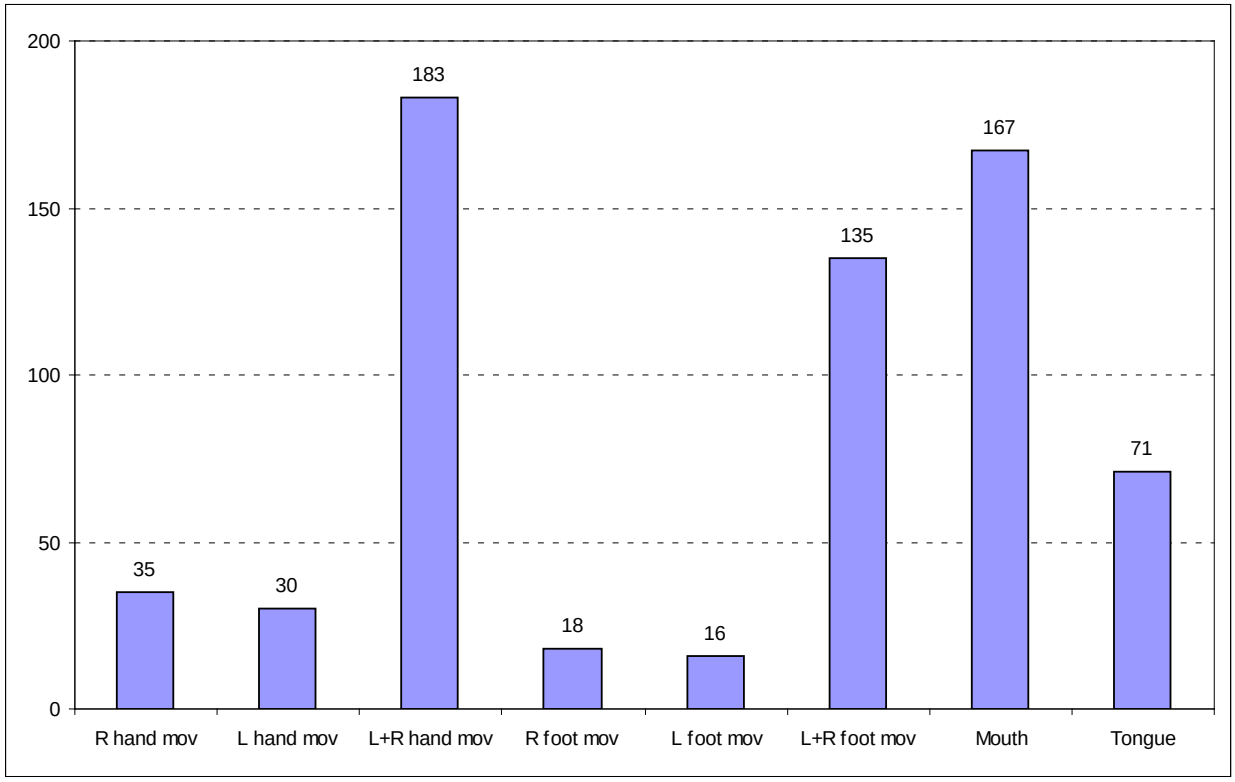

Figure 2. Motor tasks performed by patients during fMRI study. The same tasks were subsequently replicated during surgery.

EEG and EcoG. EEG-ERPs: 32 channels Neuroscan system. Elastic cap with 21 electrodes in standard locations (10/20 system) and 8 additional electrodes on central-parietal region (4 right and 4 left). EEG: Band-pass filter, 1.6 Hz – 100 Hz; sampling frequency, 1000 Hz. ERPs: Band-pass filter: 6.0 Hz – 300 Hz, sampling frequency 5000 Hz. Electrode position digitized by Polhemus electromagnetic tracker. ECoG: 8 platinum contacts strip (AD-TECH@, diameter 3.2 mm, inter-electrode distance, 10 mm). Source calculation (moving dipole method): Curry@ 4.5 software.

Surgical procedure. During surgery, craniotomy was performed under local anaesthesia in awake patients, according to lesion location, controlled "on the field" by a neuronavigation system (Medtronic) serving also to determine the location of the multielectrode device. Before cortical penetration, the microelectrode array position was online adjusted according to the tumor border, to patient's fMRI and to hr-EEG. During surgery, the same tasks previously tested during the fMRI session were performed by the patient and the neuronal activity was acquired by a custom designed software and stored on a computer for the successive analysis.

Particular attention was paid when lesions were close to motor, premotor and frontal speech-related cortices, as shown by fMRI. In these cases, after an accurate mapping of the cortical motor properties by surface electrical stimulation (bifasic, constant current, 0.5-4 mA, 100 Hz), patients were required to execute active movements of body parts close to the lesion (in terms of somatotopy), observation of similar movements performed by other individuals (to activate the motor system through mirror neurons) and verbal tasks involving speech production and speech listening.

Single Neuron Electrophysiology.

To optimize the microrecording procedure and to allow us to collect as much data as possible during the limited period of time allowed by surgery (approximately 40 min/session), recordings are performed with an 8 channels multielectrode device. Microelectrodes are arranged according to a linear array (distance between electrodes, 2.5 mm) and are driven in the cortical depth with a resolution better than 10 microns. The recording system can be positioned according to surgical needs (lesion site), taking care, however, that the position of the microelectrode array is in correspondence of the anatomic lesion border, previously determined by nuclear magnetic resonance. The precision of array localization is granted by an optical system tracking the 3-D position of active infrared markers attached to the microelectrodes array.

The microdrive used for single neuron recordings was kept in place by an articulated arm acutely attached to the border of the craniotomy by means of a holding screw. The microelectrodes (Tungsten, epoxy insulated, shaft diameter 250um, tip diameter <10um) are held by individual sockets attached on a high-precision linear slide (IKO Nippon Thompson) mobilized by one single motor. The microdrive has been realized in collaboration with IIT. It is fully steam sterilizable and equipped with a piezoelectric linear motor (Physic Instruments) actuated in closed-loop. The position sensor is a high-temperature resistant optical encoder (Mercury). This new microdrive associates a very precise positioning of the microelectrodes (< 1um) with a high velocity of mobilization (>500 mm/s). The neural discharge picked up from microelectrodes was amplified (x1000) by a specially designed microchip characterized by low-noise (<2 uV) and low-power properties. Note in the green small panel the microelectrodes tip protruding from a sheet of silicon sponge used to contrast the brain pulsations. All system

components are powered from batteries and, because of electrical isolation, it is safe from accidental current discharges. The acquired signal quality is comparable to the best commercial multichannel systems used for animal experiments in laboratories (see RESULTS) while the simplicity of the set-up makes it suitable for a use by medical staff with a minimal training. We successfully tested this system in human surgery room. Laboratory tests show that such a system is relatively easy to scale to up to 64 channels.

System blocks

1) The head-stage block contains

a) an 8-channel integrated amplifier chip,

b) two motor drives- one for electrode positioning and the second for the manual control of the pressure applied to the brain to prevent excessive bulging

c) an optical sensor that tracks the electrode position.

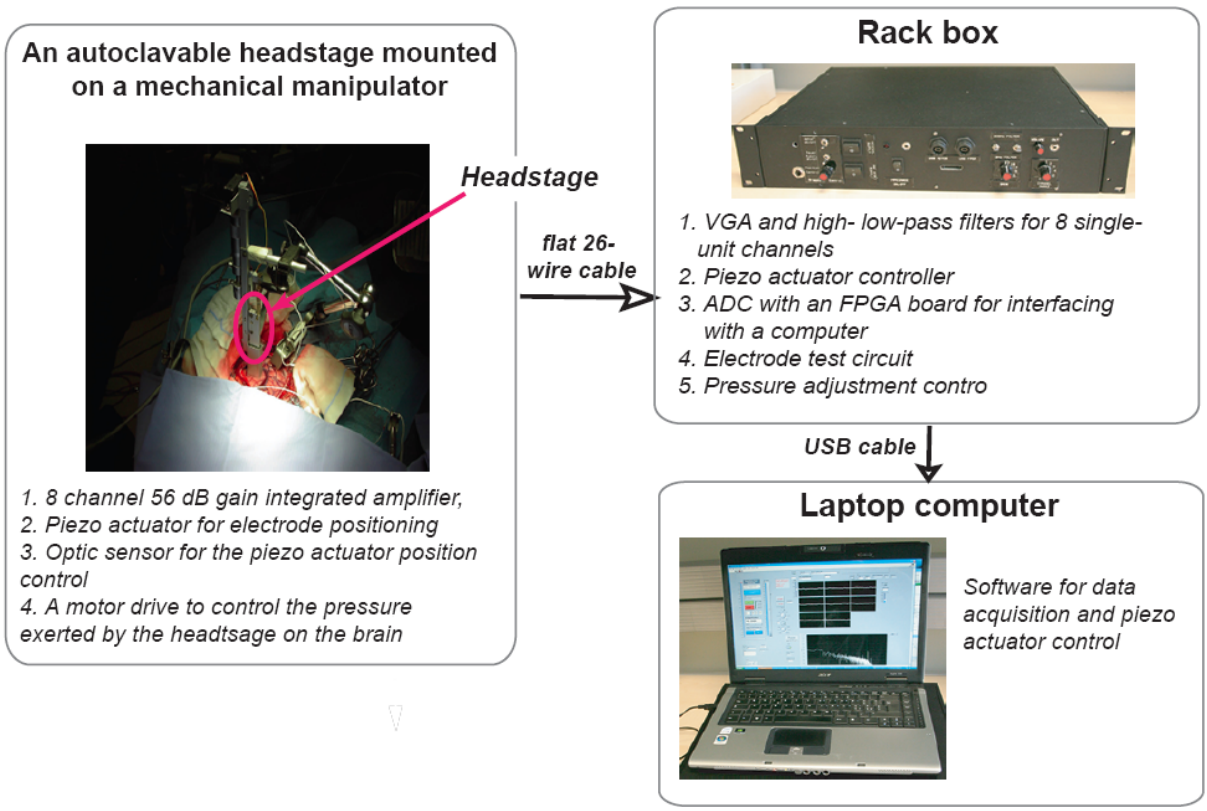

Figure 3. Scheme of three major blocks of the recording system.

A flat 26-wire cable exits the head-stage and is used for connection to the rack control unit. The head-stage including the connection cable can be autoclaved.

2) The rack control block contains:

a) One signal conditioning board (high- and low-pass filters, audio buffers, a multiplexer and an analog-digital 10 bit converter),
b) One FPGA board for interfacing of digital electrode data with a computer,
c) A commercial controller C-865 (Physics Instruments, Germany) for electrode position control that drives the piezo-actuator P661.P1 (Physics Instruments, Germany) and receives the electrode coordinate data from the Mercury 2000 optical sensor,
d) A control board for manually adjusting pressure

3) The portable computer is connected to the control unit via a USB cable. The computer employs a LabView based custom-written software for electrode data acquisition and to control the electrode position.

The system performs two main functions: acquires the single- and multi-unit signals from 8/16 electrodes and moves the electrodes into the patient's brain. Since the data acquisition system is relatively independent from the electrode movement control and has been designed by us, a brief description is presented below. In contrast, the motor control is largely based on off-shelf components except for the head-stage itself, thus only the head-stage design is discussed in more detail.

Headstage

Probably one of the most technologically complex components of our system is the headstage. During the design process, we wanted to meet the following requirements:

a) the headstage preamplifier should provide sufficient signal amplification to permit long (~5m) cables between the headstage and the rack, the same requirement should be applied to all wires of mechanical controls;
b) the weight should not exceed ~100 g because of the fragility of the manipulator that has to be mounted on the patient's skull,
c) all parts should be heat- and humidity-resistant because the whole headstage should be autoclavable (20 min 120 °C, steam saturation);
d) the mechanical drive should move electrodes and report their position;

e) the pressure exerted on the brain by the headstage should be manually controllable so that the excessive brain tissue bulging and pulsation is avoided.

Our headstage (see Figure below) meets all these requirements. For example, the below-described 8-channel integrated pre-amplifier employed in the headstage PC board provides a 56 dB gain that is sufficient to ensure that no noise is introduced via the connecting 5 m cable. Meanwhile, because of employment of an integrated chip, the board has very few components and all of them can withstand temperatures of up to 125°C. The piezo actuator for the electrode positioning can withstand such high temperatures (up to 180°C, www.piceramic.com/site/piezo.html).

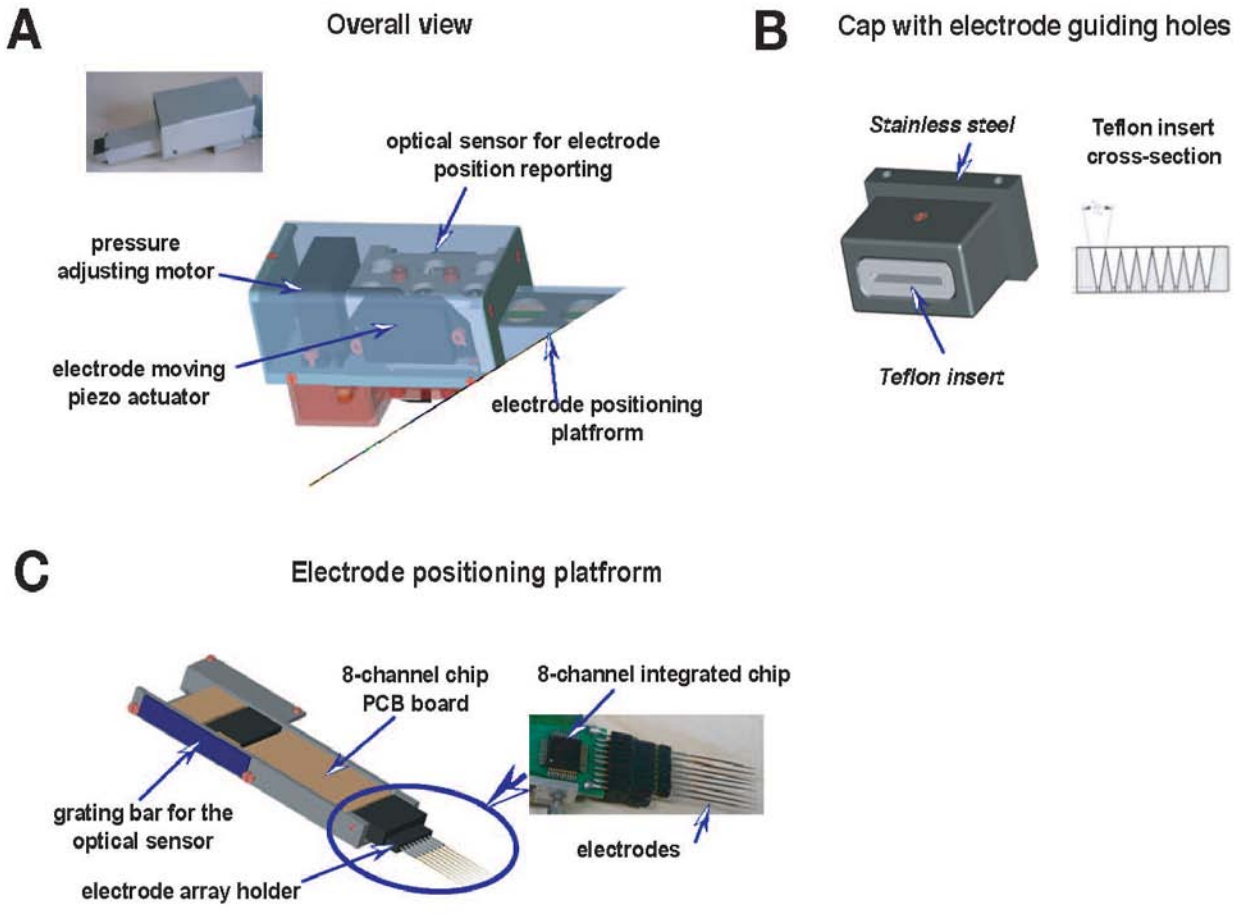

Figure 4. *A*. The overall view of the headstage with its major components. *B*. The cap is used to apply pressure to the patient's brain to prevent excessive bulging and to guide electrodes into their appropriate positions. *C*. The electrode moving platform contains both the electrode holder and the pre-amplification board with the 8-channel integrated amplifier chip.

Weight (~100g) and dimensions (115 X 35 X 38 mm) were reduced by accurately designing all the parts and by employing aluminum wherever possible except for the cap (Fig. 2B), which comes in direct contact with the human brain, made of stainless steel hosting a Teflon insert that has conical holes to facilitate electrode insertion.

The electronic board fits inside of a narrow aluminum frame shielded by a thin aluminum alloy cover (Fig. 2A and C). The whole frame (Fig. 2C) is moved by a piezo actuator P-661.P01 controlled remotely from a computer. Since electrodes are inserted directly into the board connector, there is little interaction between the input and the output of the integrated chip. A Mercury 2000 optical sensor is used for detection of the precise frame position. The whole loop formed by the piezo-actuator and the sensor is managed by C-867 controller (Physics Instruments, Karlsruhe/Palmbach, Germany) commanded from a computer.

To avoid an excessive brain tissue bulging in the skull opening due to heart pulsations in an open brain portion of the patient, an adeguate, manually controlled pressure has to be applied. To this end, the whole structure can be moved by a small motor (Fig. 2A) controlled manually from the rack.

Recording system

The overall block diagram of the recording system is shown in Fig. 5A. A more detailed description follows below:

The electrode signals are amplified by an 8-channel integrated circuit designed at the Politecnico di Milano, Italy, that contains 8 identical low-noise amplifiers (LNA) with output buffers. These integrated pre-amplifiers, similar in circuit design and performance to the prototypes presented by the same authors previously (Borghi et al. 2008; Bonfanti et al. 2009), were designed to fulfill the stringent requirements that are applied to the front end of the neural signal acquisition system. Here is the list of such requirements that are met in our integrated amplifier:

1) to prevent the saturation of the amplifier output, the dc offset generated by the electrode-tissue interface has to be eliminated;

2) to minimize the noise added to the recorded signal by the amplifier, the input referred noise of the amplifier has to be lower than a typical electrode background noise of 5 μV - 10 μV rms ;
3) the amplifier should provide a first preliminary band-pass filtering for neural signal, i.e. from few Hz to 5-10 kHz;
4) to minimize the interference from 50-60 Hz, the amplifier should have a high common mode rejection;
5) to minimize the contribution to the noise from the subsequent amplification stages, the amplifier should provide a sufficient gain factor,
6) to minimize the interference from the external sources in the cable connecting the headstage to the signal conditioning board, the amplifier should provide a low impedance output.

Each pre-amplifier has three stages. The first stage is an ac-coupled high-pass filter, employing subthreshold PMOS transistors in the feedback path that synthesize a high value resistance. The mid-band gain is set to –67 by the ratio of two capacitances, C_1/C_2, while the high-pass pole is set below 10 Hz just to reject the dc offset and the voltage drift of the electrode. A G_m-C high-pass filter with a tunable cut-off frequency (from few Hz to 1kHz) is inserted after the first stage: by removing local field potential, it permits to tune the bandwidth for action potentials. In addition, it prevents the saturation of the overall preamplifier by large signals in the local field potential band. Last, a second gain stage is added after the high-pass filter to provide a further amplification and low-pass filtering. It's a single-ended capacitive-coupled voltage amplifier with a gain of 34 achieved with C_3=5 pF and C_4=150 fF, and a low-pass cut-off frequency of about 15 kHz. Thus, the overall pre-amplifier gain is about 2200, with a tunable high-pass filtering and a 15-kHz low-pass cut-off frequency.

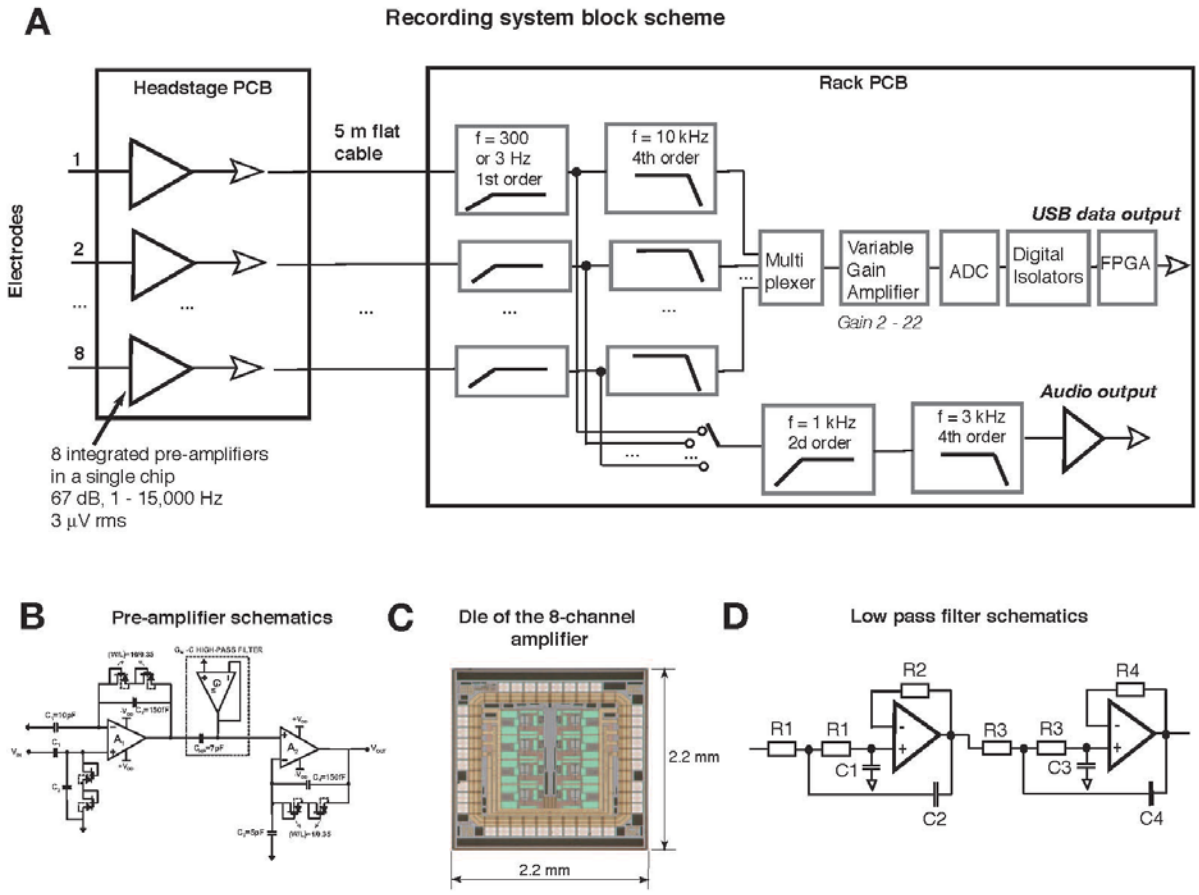

Figure 5. A. Block diagram of major electronics blocs in the signal processing chain. B. Gross schematics of a single amplifier of the 8-channel integrated amplifier chip. C. Microphotograph of the integrated chip die. D. Gross schematics of a 4th order filter that was used in the signal conditioning board.

Since the noise properties of the whole pre-amplifier are mainly determined by the operational amplifier of the first stage (A_1), in this stage we adopted a telescopic cascode amplifier that, thanks to its few components, permits to attain low-noise with a low-power consumption (see (Borghi et al. 2008) for details).

The amplified signal is sent to a class AB voltage buffer that is used to lower the output impedance to less than 1 KOhm and to drive the 5 m flat cable that runs from the amplifier to the rack containing the conditioning board.

The power consumption of each pre-amplifier is about 13.5 μW for a power supply of 3 V- 12 μW for the first stage and 1 μW for the second stage while the power consumption of the G_m cell is negligible. In addition, each output buffer draws 10 μA resulting in a power

consumption of 30 μW). The input referred noise is about 3 μV rms in the 10 Hz – 15 kHz band, that reduces to 2.2 μV rms for a 300 Hz – 10 kHz band.

The 8-channel integrated circuit was implemented in 0.35-μm AMS CMOS technology (the die is shown in Fig. 3C) and packaged in a TQFP48 package. Since no additional components are required for the integrated 8-channel chip functioning, the headstage electronics board is very compact, 12 X 15 mm^2. In our laboratory we also used a 16-channel version of the headstage board of the same size with two chips mounted on both sides of the board. Thus, the number of channels can be easily doubled if an appropriate electrode holder is used.

Signal conditioning board

Electrode signals amplified at the headstage are then sent to the signal conditioning board located in the rack box (see Fig. 3A). The signal conditioning board serves four main purposes.

First, the board performs an additional filtering, both high-pass and low-pass. The high-pass filter is a first-order filter with a selectable cut-off frequency that can be either 300- or 3-Hz. A higher cut-off frequency is necessary to remove local field potential (LFP) signals and the 50-Hz interference that often is present in the amplified signal while the lower cut-off frequency is used for multi-unit/LFP data acquisition. The low-pass fourth order 10-kHz Butterworth filter has a 10 kHz cut-off frequency (Fig. 3D). This filter leaves unmodified the recorded action potentials while sufficiently reducing the high frequency range to eliminate the alias noise that might occur during the multiplexing and digitization step that has a typical working frequency of 40 kHz. Such a high sampling frequency ensures high quality of the acquired signal while current computer power has no problems to process the increased amount of data points.

Second, the signal conditioning board provides a properly filtered and amplified audio output. This output is necessary for surgeons trained to distinguish the presence of neuronal activity by listening to the recorded sound. Thus, using software or electronic switch one can select a channel for further band-pass filtering (a second order 1-kHz high-pass and a fourth order 3-kHz low-pass Butterworth filters) and send the amplified signal to a loudspeaker.

Third, on the board, the 8 amplifier signals are multiplexed, digitized by a 10-bit AD converter and then appropriately encoded for interfacing with a computer via USB connection.

A commercial FPGA from Opal Kelly (Portland, OR, USA) based on Xilinx Spartan-3E integrated chip was used for processing of the digital multiplexed signal. An analog multiplexing of 8 channels was preferred to an ADC per channel the subsequent digital management of 8 digital channels. Such a choice reduced the number of AD converters, simplifying the signal conditioning board. The only drawback of this solution is an increased cross talk between the adjacent channels that, however, according to our measurements, remained at acceptable –40 dB levels.

Fourth, the conditioning board performs signal isolation that is mandatory for the safety reasons, i.e. to isolate a patient from the laptop that may be connected to the power line and be the source of unexpected electric discharges. To this end, a digital isolator was inserted between the AD converter and the FPGA. This isolation also disrupts the current loop that may be formed by the patient, the headstage, the acquisition system and the laptop due to the presence of ground wires. Thus, in addition such an electrical isolation reduces the 50-Hz noise and other magnetic interferences.

Acquisition software

The software was written employing the LabView environment but it can be installed as a stand-alone program. A sample screenshot is shown in Fig. 4. The program window can be divided in two sections, one devoted to electrode position control and the second to the of electrode generated data stream.

The main functions of the latter part are:

1) decoding the digital multiplexed signal that arrives from the signal conditioning board by organizing it in 8 independent data streams at 20 – 40 kHz sampling rate and 10 bit resolution;

2) displaying all data streams in a continuous mode on a computer screen;

3) saving the desired sections of data;

4) adding digital filtering to the displayed and recorded data (both high-pass and low-pass tunable filters are available).

Each display channel can be zoomed for a better visualization of acquired data. The duration of the displayed trace is set by the user. In addition, a software based audio channel selection is available and a frequency power spectrum that is very useful while identifying the noise sources and for LFP analysis.

The electrode position control has buttons for defining the '0' coordinate ('home' position), the step size for electrode movement and the velocity at which the electrodes are moved. There are indicators for the electrode location and the velocity at which they are moved.

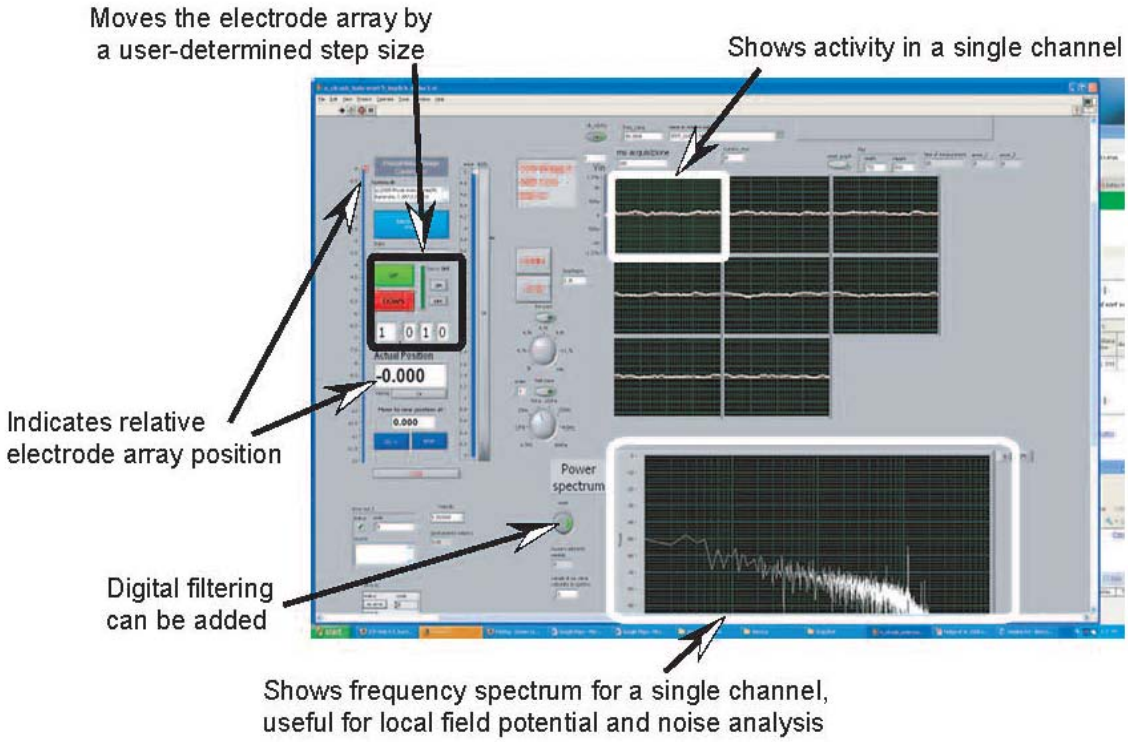

Figure 6. The screenshot of the acquisition software

3 Results

Preliminary testing.

Before entering the surgery room, the system was extensively tested by performing single neurons recordings from anesthetized rats. These tests helped to optimize the system for stability and high signal quality under diverse conditions. Special care was taken to achieve high reliability and simplicity of use, both so important during surgery.

Direct comparison with the Plexon (Dallas, Texas, USA) MAP system showed that the noise levels and distortions introduced by our amplifier chain is minimal (Fig. 5). In fact, in the signal band of 0.3 – 7 kHz, the noise levels are almost identical in our and the MAP systems. For instance, for a recording shown in Fig. 5A, the noise level was 8.3 μV rms for our trace while it was was 8.9 μV rms for the trace obtained with the Plexon MAP instrument.

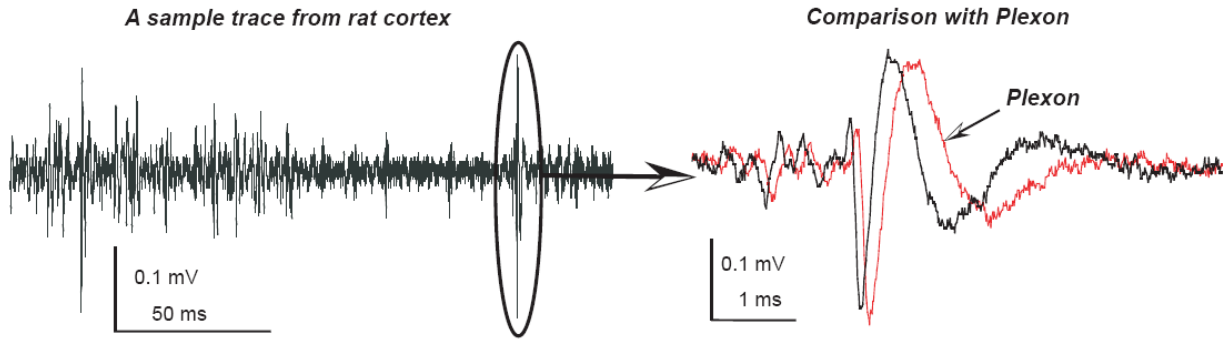

Figure 7. Neural traces recorded by our system during preliminary testing. Tests showed that even weak single units (~ 30 microV Vpp) can be detected and the parallel recording with a Plexon comercial system shows minimal differences between the signals attained with our system and with Plexon 32 channel commercial set up.

The bench top tests showed that the noise of the whole system with all connections was below 3 μV rms in the 0.3 – 7 kHz band that is similar to the specs of the MAP system (below 5 μV rms according to the datasheet or ~ 3μV rms according to our measurements).

The Figure below shows a typical multichannel recording from human premotor cortex. Note the spikes and the quite satisfying signal-to-noise ratio.

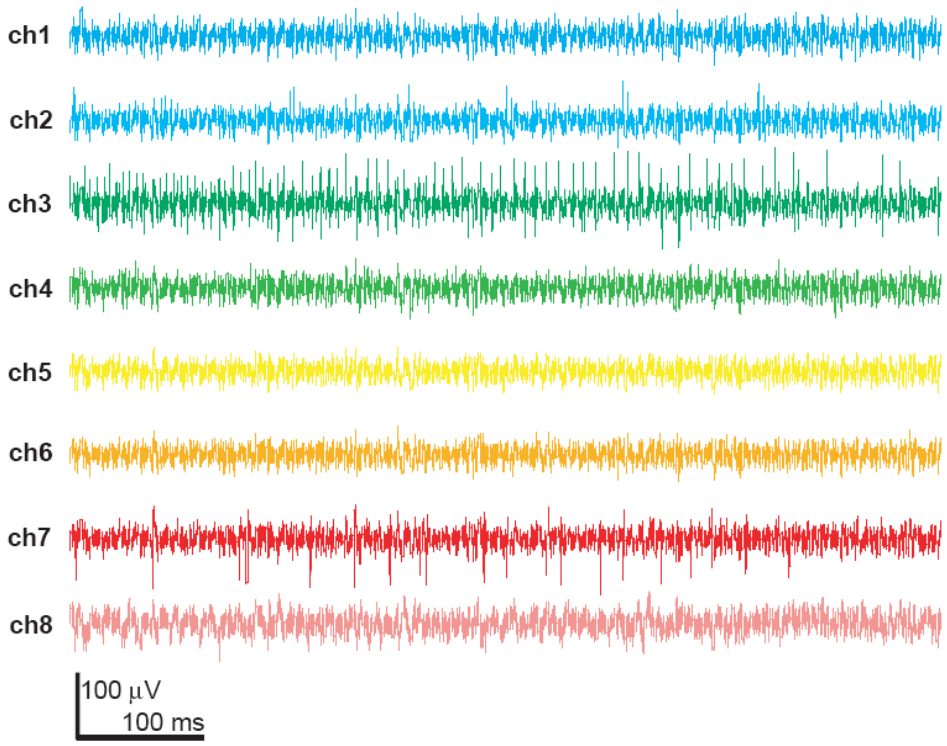

Human recordings.

Before undergoing surgery, all the patients were neuropsychologically tested and were submitted to fMRI sessions where gross brain activity was acquired. During fMRI each patient was requested to perform a series of tests selected from a library of ready procedures, according to the site of her lesion.

The figure below shows a typical result of fMRI evaluation of wrist (red) and ankle (blue) mobilization. Note the proximity to the hand motor spot of the tumor of this patient. Twenty-four patients already underwent fMRI control sessionsafter recovery from surgery (1-3 months).

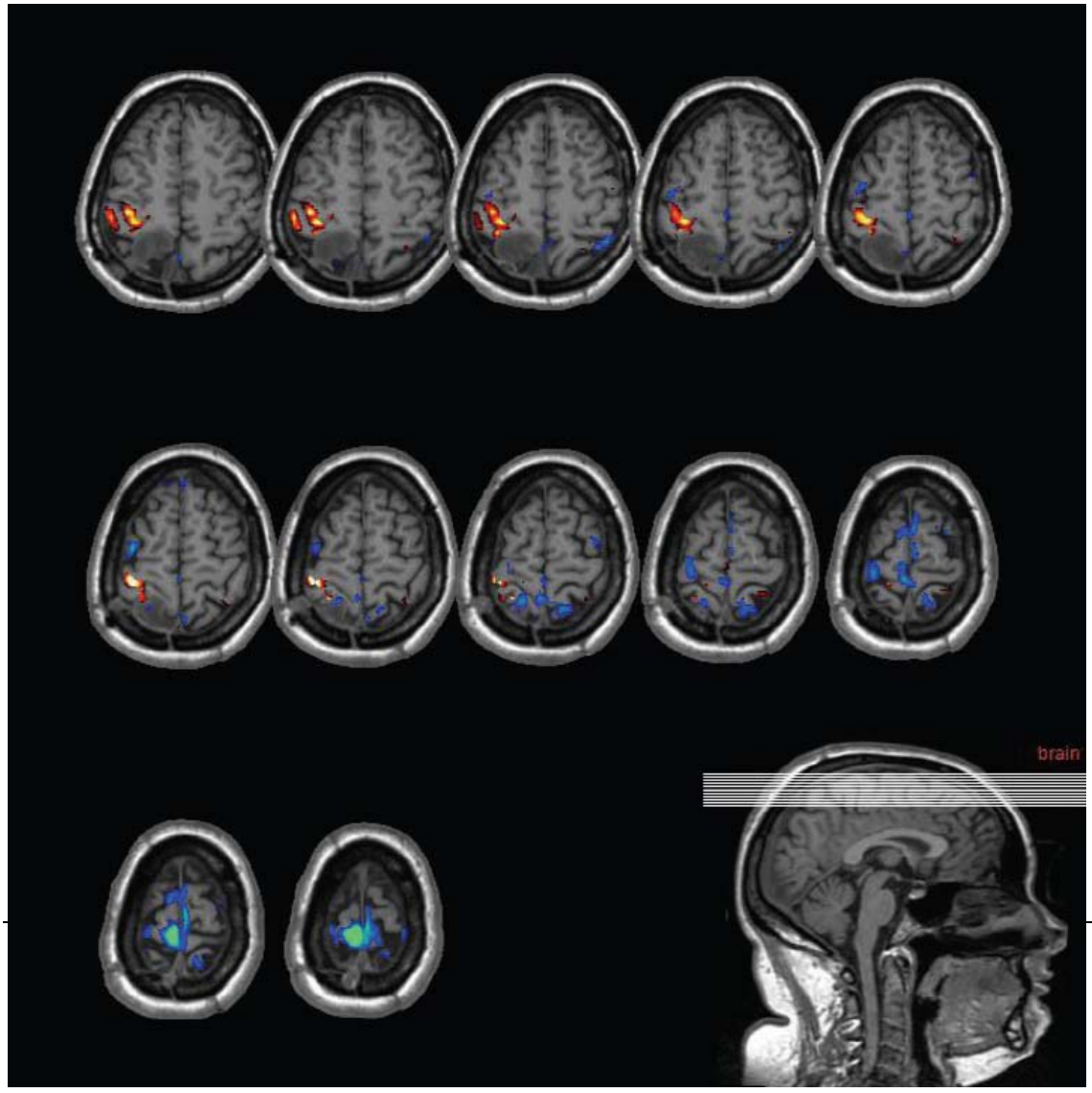

Figure 8. Results of a typical fMRI acquisition. Wrist (blue-green) and ankle (red-yellow) activations are shown. The color code is related to the statistical significance of the activation.

In addition to fMRI, a pre-surgical EEG evaluation was performed in the large majority of patients as well. Frequently, there was a nice spatial superimposition between the reconstructed EEG dipole as acquired during, e.g., wrist mobilization or median nerve electrical stimulation, and the fMRI activation related to the same effector.

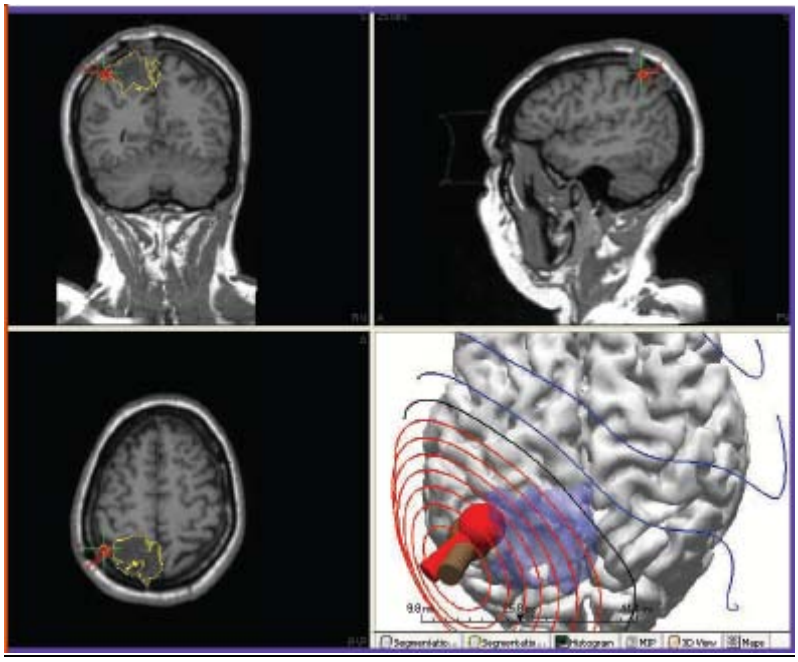

Figure 9. Electrophysiological localization of the N30 dipole following electrical stimulation of the median nerve at wrist. Note the quite good spatial correspondence with the fMRI data shown on the left. ERPs dipoles are always deeper (slightly but significantly) than the peaks of BOLD signal shown by fMRI. This may partially be due to the vascular nature of the BOLD activation.

After this preliminary testing, the patient was submitted to the surgery session. The figure below (Figure 10) resumes all the data characterizing a typical session. Figure 11 shows some recordings performed at the border of the tumor (the dark gray parietal area shown in Figure 10, A.

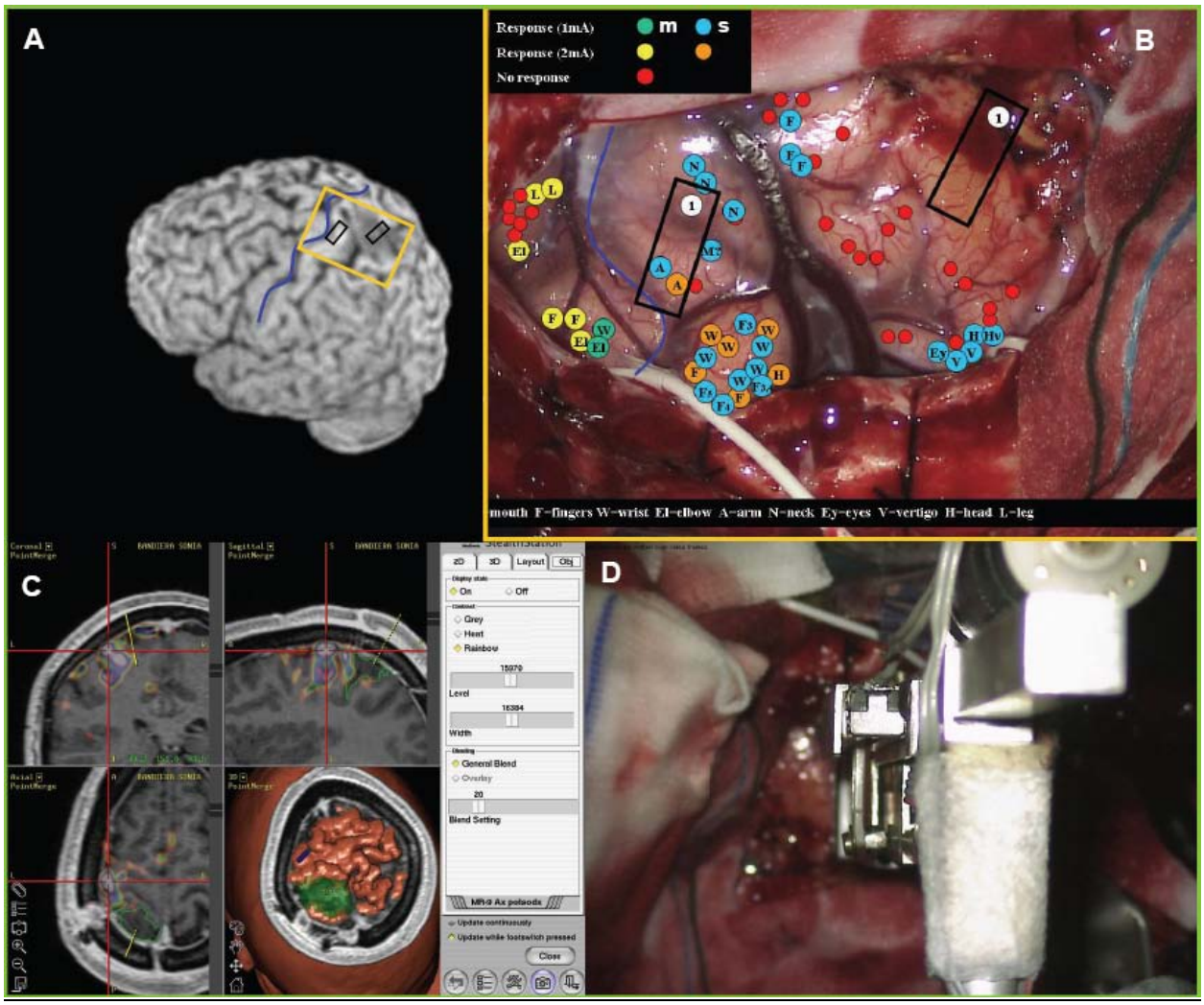

Figure 10. Cortical mapping during neurosurgery. A, tridimensional reconstruction of the patient's brain (BET function, MRIcro software). The lesion (dark gray area within the yellow rectangle) is visible in the left parietal cortex. The central sulcus is marked by a blue line in both panels, A and B. B, the operatory field. The location of sites from where motor (m) and sensory (s) responses were evoked by surface electrical stimulation at two different current intensities (1 mA and 2 mA) are shown by coloured labels. The two black rectangles indicate the location of the microdrive head during the two single neuron recording sessions. The label (1) inside each rectangle shows the position of the microelectrode #1. C, neuronavigation data used during surgery. The lesion location (green), the fMRI activation during wrist mobilization (blue-purple scale) and the location of the microdrive head are shown. D, an enlarged view from above of the microdrive head positioned on the cortex (location: leftmost black rectangle shown in panel B).

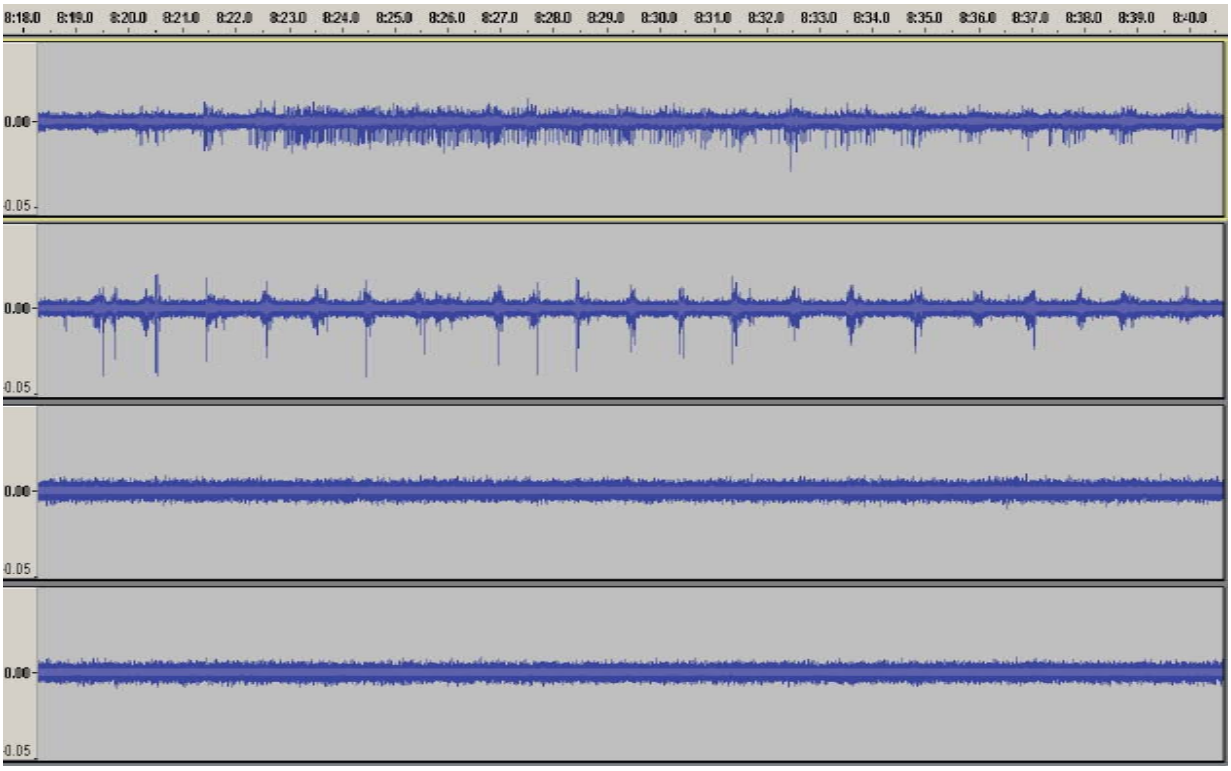

Figure 11. High impedance (0.5-1 MΩ) single neuron activity recorded during 22 s from the rightmost location depicted in panel B (operatory field). All the microelectrodes are recording from the pathologic tissue. Note the presence of rhythmic activity in electrode #1 and #2 (pathologic bursts) and the absence of spikes in electrodes #3 and #4. The frequency of rhythmic activity (about 1 Hz) was unrelated to physiological parameters such as respiratory or heart rates. Recording sessions lasted about 30 minutes allowing a sufficient comprehension of the functional properties of the recorded cortex.

3 Conclusions

This deliverable shows the feasibility of a multimodal approach to intra-operatory functional mapping of the human cortex in awake and collaborative patients. These are the main achievement of this study, which is currently still ongoing:

1) Intracortical single neuron recordings have been shown to represent a critical tool to provide strategic information to the surgeon in order to localize the functional border of brain tumours contiguous to primary motor, premotor, speech-related and primary somatosensory cortices. This is particularly true for the case of low-grade gliomas which are characterized by a poorly defined infiltrated border.

2) The possibility to record from the healthy nervous tissue, bordering the pathologic region, provides neurophysiologists with several new and fundamental information on how the human brain works. Among the functions that have been investigated the relationship between language and action representation, the perceptual correlate of proprioception and the study of the granularity of the somatotopy are those providing the more interesting information. This is particularly interesting in the framework of the study of sensorimotor properties of human neurons.

3) The preoperative investigation with fMRI, neuropsychological testing and ERPs allows to correlate single neuron properties with the results of different techniques characterized by different spatial and temporal resolutions.

5 References

Asano E, et al. "Origin and propagation of epileptic spasms delineated on electrocorticography." Epilepsia 2005; 46(7): 1086-97.

Berger MS, et al. "Low grade gliomas associated with intractable epilepsy: seizure outcome utilizing electrocorticography during tumor resection." J Neurosurg 1993; 79: 62-69.

Berger MS and Rostomily RC, "Low grade gliomas: Functional mapping resection strategies, resection strategies, extent of resection, and outcome." J Neuro-Oncology 1997; 34: 85-101.

Bonfanti A, et al. "A Low-Power Integrated Circuit for Analog Spike Detection and Sorting in Neural Prosthesis Systems." International Conference on Biomedical Electronics and Devices (BIODEVICES 2009), Porto (Portogallo). 2009.

Borghi T, et al. "A Power-Efficient Analog Integrated Circuit for Amplification and Detection of Neural Signals." International Conference of the Engineering in Medicine and Biology (EMBC 2008), Vancouver (Canada) 2008.

Duffau H, et al. "Usefulness of intraoperative electrical subcortical mapping during surgery for low-grade gliomas located within eloquent brain regions: functional results in a consecutive series of 103 patients." J Neurosurg 2003; 98: 764-768.

Fadiga L, et al. "Visuomotor neurons: ambiguity of the discharge or 'motor' perception?" Int J Psychophysiol 2000, 35:165-77.

Guthrie BL and Laws ER. "Supratentorial low-grade gliomas." Neurosurg Clin N Am 1990; 1: 137-48.

Nakamura M, et al. "Analysis of prognostic and survival factors related to treatment of low-grade astrocytomes in adults." Oncology 2000; 58: 108-116.

Neuoloh G, et al. "Motor evoked potential monitoring with supratentorial surgery." Neurosurgery 2004; 54(5): 1061-72.

Ng Y-T, et al. "The role of neurosurgery in status epilepticus." Neurocrit Care 2007; 7: 86-91.

Okun, M., M. Tagliati, et al. "Management of referred deep brain stimulation failures." Arch Neurol 2005; 62(62): 1250-55.